arXiv:1105.5204v1 [physics.atom-ph] 26 May 2011

Attosecond probing of instantaneous AC Stark shifts in helium atoms

Feng He[1,2]*, Camilo Ruiz[3], Andreas Becker[4], and Uwe Thumm[5]
[1]*Key Laboratory for Laser Plasmas (Ministry of Education) and Department of Physics, SJTU, Shanghai 200240, People's Republic of China*
[2]*Max-Planck-Institute für Kernphysik, Saupfercheckweg 1, D-69117 Heidelberg, Germany*
[3]*Centro de Laseres Pulsados CLPU, Plaza de la Merced s/n E-37008 Salamanca, Spain*
[4]*Department of Physics and JILA, University of Colorado, Boulder 80309-0440, USA*
[5]*James R. Macdonald Laboratory, Kansas State University, Manhattan, Kansas 66506, USA*

(Dated: January 25, 2013)

Based on numerical solutions of the time-dependent Schrödinger equation for either one or two active electrons, we propose a method for observing instantaneous level shifts in an oscillating strong infrared (IR) field in time, using a single tunable attosecond pulse to probe excited states of the perturbed atom. The ionization probability in the combined fields depends on both, the frequency of the attosecond pulse and the time delay between both pulses, since the IR field shifts excited energy levels into and out of resonance with the attosecond probe pulse. We show that this method (i) allows the detection of instantaneous atomic energy gaps with sub-laser-cycle time resolution and (ii) can be applied as an ultrafast gate for more complex processes such as non-sequential double-ionization.

PACS numbers: 42.50.Hz, 32.80.Rm

The energetic shift of atomic levels in external electric fields is a well-known phenomenon and usually referred to as "Stark shift". For static fields that are much weaker than intra-atomic Coulomb fields, Stark shifts can be calculated using perturbation theory [1]. For oscillating external fields in the optical and near-IR range, perturbation theory breaks down at intensities of $\approx 10^{12}$ W/cm^2 [2], orders of magnitudes below the peak intensities available in state-of-the-art ultrashort laser laboratories. If such strong external fields are maintained over many optical cycles, cycle-averaged level shifts can be evaluated, e.g. by exploiting the quasi periodicity of the external field using the non-perturbative Floquet theory [3–5]. However, for the recently developed strong few-cycle IR laser pulses [6–10], atomic level shifts are non-perturbative in nature and also render the continuum-wave Floquet picture inapplicable.

Modern pump-probe experiments combine extended ultraviolet (XUV) attosecond pulses of sub-IR-cycle pulse lengths (1 as = 10^{-18} s) with phase-coherent IR laser pulses to observe electronic dynamics in atoms, molecules and solids [11–16]. The role of laser-dressed highly excited energy levels in atomic excitation and ionization has been studied recently using attosecond technology [17, 18]. In this Letter, we show that the attosecond pump-probe technique should also enable the measurement of *instantaneous* level shifts of low lying bound atomic states in alternating optical electric fields. Further, we demonstrate how the control of instantaneous level shifts can be exploited to gate other strong-field phenomena, such as non-sequential double ionization (NSDI).

To this end, we simulate an XUV pump - IR probe scenario. We choose IR laser fields with negligible distortion of the ground state of He, that are, however, strong enough to couple low excited and continuous states, inducing noticeable level splitting, shift, and decay. For the XUV pulses we fix the number of cycles and vary the central frequency of the pulse. Key to our investigation is the observation that, for a given central frequency ω_{SA} of the single attosecond (SA) pulse and depending on the delay Δt between pump and probe pulse, the IR pulse may shift low-lying bound states into or out of resonance with one-photon excitations from the He ground state. The excited atom may then be easily ionized by the IR pulse. If the SA pulse is applied while the instantaneous level energies are off (in) resonant with ω_{SA}, less (more) excitation and thus less (more) ionization out of excited states is expected to occur. This suggests that detection of the ionization probability as a function of ω_{SA} and Δt can be used to track the instantaneous Stark shifts.

We will analyze this strategy by modeling He in the so-called single-active-electron approximation (SAEA), in which the time-dependent Schrödinger equation (TDSE) in velocity gauge reads (unless indicated otherwise, we use Hartree atomic units, $e = m = \hbar = 1$):

$$i\frac{\partial\Psi(z,\rho;t)}{\partial t} = \left[\frac{(p_z - A(t)/c)^2 + p_\rho^2}{2} + V(z,\rho)\right]\Psi(z,\rho;t), \tag{1}$$

where z and ρ are cylindrical electronic coordinates parallel or perpendicular to the laser-polarization axis, respectively, and p_z and p_ρ are the corresponding conjugate momentum operators. $A(t) = -c\int dtE(t)$ is the vector potential associated with the XUV and IR laser fields and c the speed of light. $V(z,\rho)$ models electronic

---

*fhe@sjtu.edu.cn

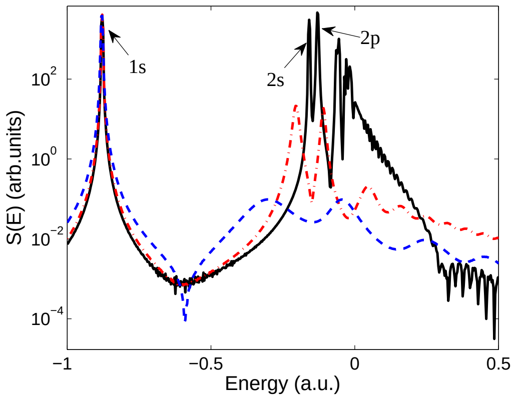

FIG. 1: (Color online) Energy levels for He, calculated in SAEA without (black line) and with static external electric fields with intensities of 10^{13} W/cm^2 (red dash-dotted line) and 10^{14}W/cm^2 (blue dashed line).

correlation in terms of screening of the nuclear Coulomb potential by the passive electron [19].

For later reference, we first compute energy-level shifts in the static field E_{st} in the length gauge. Fig. 1 shows the spectrum $S(E)$ of He atoms without external field and in static fields with intensities of 10^{13} and 10^{14}W/cm^2, calculated by Fourier transformation of the autocorrelation function, $S(E) = |\int dt\langle\psi(t)|\psi(0)\rangle e^{-iEt}|^2$ [20]. At these intensities the ground state is nearly unaffected by the external static field, while the excited $2s$ and $2p$ states are shifted to lower and higher energies, respectively [21]. The level spacing $E^{(\mathrm{static})}_{1s,2s}$ between the field-shifted $1s$ and $2s$ levels decreases with increasing E_{st}, while $E^{(\mathrm{static})}_{1s,2p}$ increases.

Exposed to the combined electric field of a SA pulse and a delayed IR pulse $E_{IR}(t)$

$$\begin{aligned} E(t) &= E_{SA}\sin(\omega_{SA}t)\exp\left[-2\ln 2\left(\frac{t-\Delta t}{\tau_{SA}}\right)^2\right] \\ &\quad +E_{IR}\sin(\omega_{IR}t)\cos^2\left(\frac{\pi t}{\tau_{IR}}\right), \end{aligned} \tag{2}$$

with $E_{IR} = 0$ if $|t| > \tau_{IR}/2$, level shifts induced by $E_{IR}(t)$ can be probed on an attosecond time scale. We choose Gaussian SA pulses with an intensity of 2×10^{13} W/cm^2, a pulse duration τ_{SA} (FWHM) of two XUV cycles, and variable ω_{SA}, and a cos^2-shaped IR laser pulse with a central wavelength of 800 nm, an intensity of 3×10^{14} W/cm^2, and a pulse duration τ_{IR} of four IR cycles. We neglect the spatial intensity profile of the IR laser pulse since SA pulses can be made to only overlap with the spatial center of the IR pulse [22, 23].

We calculate the ionization probability of He in the oscillating field, Eq. (2), by propagating Eq. (1) on a numerical grid with equidistant spacings $\Delta z = \Delta\rho = 0.3$ and time steps $\delta t = 0.05$. The spatial grid includes 2000

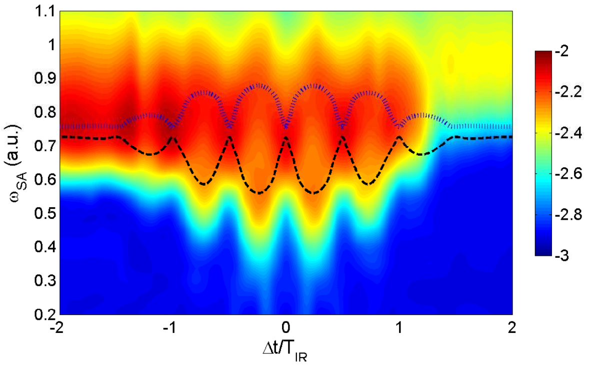

FIG. 2: (Color online) Ionization probabilities (logarithmic color/grey scale) of He calculated in SAEA as a function of the center frequency ω_{SA} of the SA pulse and time delay Δt between the SA and IR laser pulses in units of the IR laser period T_{IR}. Superimposed dashed and dotted curves show the quasi-static level spacings $E^{(\mathrm{static})}_{1s,2s}$ and $E^{(\mathrm{static})}_{1s,2p}$, respectively. Laser parameters are given in the text.

(400) points and covers the range from −300 to 300 (0 to 120) along the z (ρ) axis. We use a $\cos^{1/6}$ masking function to suppress reflections from the grid boundaries [24] and determine the single-ionization probability from the accumulated outgoing electronic current into the absorber region. The wave function is propagated until the ionization probability becomes stabilized.

The single ionization probability P_S is shown in Fig. 2. For $\Delta t < 0$ the SA pulse precedes the center of the IR laser pulse. Accounting for the large bandwidth of the SA pulse, enhanced ionization may occur, even for ω_{SA} below the ionization threshold, via excitation to a IR laser-dressed bound state followed by ionization in the remaining IR field. Single ionization is thus mediated by either the high-energy side of the XUV-pulse spectrum that extends above the ionization continuum or in a two-step process via transiently excited atoms. Since $P_S(\omega_{SA}, \Delta t)$ behaves differently for different ω_{SA}, we analyze separately three ω_{SA} intervals. In order to support our interpretations we present in Fig. 3 (normalized) ionization probabilities as functions of (a) Δt and (b) ω_{SA} fixing the other parameter to different values.

(1) For $\omega_{SA} < 0.6$ and negligible pulse-overlap ($|\Delta t| > 1.5T_{IR}$, where T_{IR} is the period of the IR field), there is no enhancement of the ionization probability. However, P_S is enhanced and oscillates in the pulse-overlap region ($|\Delta t| < 1.5T_{IR}$) as a function of Δt with period $T_{IR}/2$. P_S reaches maxima when the SA pulse is applied at maximal IR electric-field magnitudes $|E_{IR}|$ (Fig. 3(a), red-dashed line). We explain this behavior as follows. For $|\Delta t| > 1.5T_{IR}$, the energy gap between the (essentially) field-free $1s$ and $2p$ level, $E^{(\mathrm{free})}_{1s,2p} = 0.75$, is larger than ω_{SA}, and the spectral width of the SA pulse does not overlap with the $2p$ level. Thus excitation by the SA pulse is negligible. In contrast, for $|\Delta t| < 1.5T_{IR}$ the

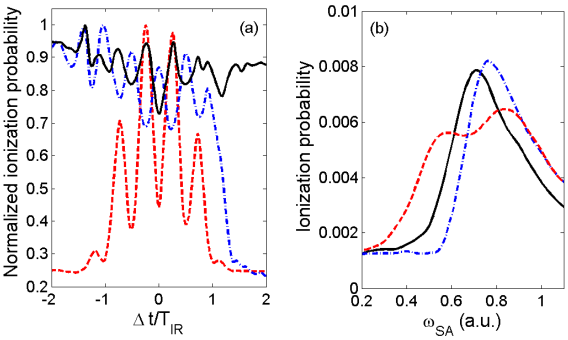

FIG. 3: (Color online) (a) Ionization probabilities, normalized to their respective maxima, as a function of Δt for three values of ω_{SA}: 0.5 a.u. (red dashed curve), 0.75 a.u. (blue dash-dotted curve), and 1.1 a.u. (black solid curve). (b) Ionization probabilities as a function of ω_{SA} for three values of $\Delta t/T_{IR}$: -2 (blue dash-dotted line), -0.25 (red dashed line), and 0 (black solid line).

dressing by the IR-laser field repeatedly shifts $E^{(\mathrm{dressed})}_{1s,2s}$ into resonance with larger values of ω_{SA}, allowing for efficient excitation followed by ionization in the IR field. The $T_{IR}/2$ oscillation of P_S indicates that $E^{(\mathrm{dressed})}_{1s,2s}$ depends on the *instantaneous* IR intensity.

(2) If ω_{SA} approximately matches the field-free energy gap $E^{(\mathrm{free})}_{1s,2p}$ and $\Delta t < -1.5T_{IR}$, excitation to the $2p$ state by the SA pulse followed by subsequent ionization via the IR pulse is very likely. In contrast, the IR pulse by itself is not able to excite and leaves the atom in its ground state. Thus, for $\Delta t > 1.5T_{IR}$, the subsequent not-IR-assisted SA pulse can only excite, but not ionize, the atom. In the overlap region ($|\Delta t| < 1.5T_{IR}$) a small-amplitude IR-laser-induced oscillation of P_S occurs. Maxima in P_S occur at vanishing instantaneous IR intensity (Fig. 3(a), blue dashed-dotted line), since the energy gap $E^{(\mathrm{dressed})}_{1s,2p}$ increases with field strength which leads to a mismatch with ω_{SA}. In Fig. 3 the blue dashed-dotted line and red dashed line have opposite carrier phases, since the corresponding energy gaps are shifted into and out of resonance with the SA frequency, asynchronously.

(3) For $\omega_{SA} > 0.8$ the spectrally broad SA pulse can directly ionize He from the ground state, leading to noticeable ionization probabilities even without pulse overlap (Fig. 3(a), black solid line). The larger ionization probability for $\Delta t < -1.5T_{IR}$ is due to dominant SA-pulse excitation followed by IR ionization, while this two-step mechanism does not apply for $\Delta t > 1.5T_{IR}$. In the overlap region $|\Delta t| < 1.5T_{IR}$, the red dashed and black solid lines are in phase due to synchronous shifts into and out of resonance with $E^{(\mathrm{dressed})}_{1s,2s}$ and $E^{(\mathrm{dressed})}_{1s,2p}$, respectively.

Further evidence for the observation of $P_S(\omega_{SA}, \Delta t)$ allowing the detection of instantaneous level shifts is obtained by comparison with the instantaneous quasi-static energy gaps $E^{(\mathrm{static})}_{1s,2s}(t)$ and $E^{(\mathrm{static})}_{1s,2p}(t)$ in the static external field $E_{st} = E_{IR}(t)$, where $E_{IR}(t)$ is the instantaneous electric field of the IR-laser pulse at time t (cf. Fig. 1). The results are drawn as dashed and dotted curves in Fig. 2 and match the contours of the ionization probability.

For a quantitative investigation, we present the ionization probability P_S in Fig. 3(b) as a function of ω_{SA} at three different delays. At $\Delta t = -T_{IR}/4$ (corresponding to a maximum of $|E_{IR}(t)|$, red dashed line) the instantaneous energy spacings can be identified by the *two* local extrema in P_S. The positions of these maxima as a function of ω_{SA} match the corresponding quasi-static energy gaps $E^{(\mathrm{static})}_{1s,2s}(t)$ and $E^{(\mathrm{static})}_{1s,2p}(t)$ for $E_{st} = |E_{IR}(t)|$ at $t = -T_{IR}/4$.

In contrast, application of the SA pulse at a zero of the IR field ($\Delta t = 0$, black solid line) leads to just one maximum in the ionization probability. The position of this maximum as a function of ω_{SA} is slightly shifted to lower frequencies as compared to the field-free energy spacing $E^{(\mathrm{free})}_{1s,2p}$ (blue dash-dotted line for $\Delta t = -2T_{IR}$ in Fig. 3(b)). This is due to the fact that the SA pulse has a finite non-zero temporal width and probes the (field-dressed) $2s$ and $2p$ levels near a zero of the IR field as well.

Understanding of the ultrafast shift of the electronic levels can be useful to control electronic transitions with a high temporal resolution. Single ionization of an atom (or a molecule) is the initial step in many strong-field processes, such as higher-order harmonic and attosecond-pulse generation, NSDI, or molecular dissociation. Our findings above suggest that these processes can be gated in a controlled way on an attosecond time scale. We demonstrate the potential of this gating technique for NSDI of He by solving the TDSE

$$i\frac{\partial}{\partial t}\Psi(Z,\overline{z},\overline{\rho};t) = \left[H_0 - \frac{P_Z \cdot A(t)}{c}\right]\Psi(Z,\overline{z},\overline{\rho};t), \quad (3)$$

within a correlated two-electron model [25], with the field-free Hamitonian

$$H_0 = \frac{P_Z^2}{4} + p_{\overline{\rho}}^2 + p_{\overline{z}}^2 + \frac{1}{\sqrt{\overline{\rho}^2 + \overline{z}^2}} - \sum_{j=1,2}\frac{2}{\sqrt{r_j^2 + s}}. \quad (4)$$

where $r_j^2 = (Z + (-1)^j\overline{z}/2)^2 + \overline{\rho}^2/4$. In this model the electronic center-of-mass coordinate Z is constrained along the polarization direction, $\overline{z}$ and $\overline{\rho}$ represent the coordinates of the (unconstrained) relative motion of the electrons parallel and perpendicular to the polarization axis, respectively. P_Z, $p_{\overline{z}}$ and $p_{\overline{\rho}}$ are the corresponding conjugate momentum operators. The soft core parameter $s = 0.135$. We solve Eq. (3) on a three-dimensional numerical grid with equidistant spacing $\Delta Z = \Delta\overline{z} = \Delta\overline{\rho} = 0.3$ and 600, 1200, and 200 grid points along the Z, $\overline{z}$, and $\overline{\rho}$ axis, respectively. To quantify the probabilities

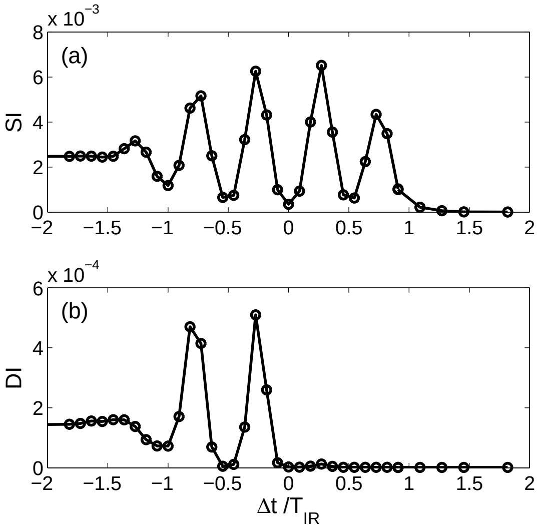

FIG. 4: Probabilities for single ionization (SI)(a) and double ionization (DI) (b) as a function of the time delay between SA and IR pulses. The SA pulse has a central frequency of $\omega_{SA} = 0.76$ a.u. and a peak intensity of $2 \times 10^{13}\mathrm{W/cm^2}$. The IR pulse has a central wavelength of 800 nm and a peak intensity of $3 \times 10^{14}\mathrm{W/cm^2}$. The simulation results (circles) are interpolated by lines.

of single and double ionization, we partition the grid as $r_1 < 12$ and $r_2 < 12$ (neutral helium), $r_i < 6$ and $r_j > 12$ ($i \neq j = 1, 2$, He^+) and the complementary space (He^{2+}) (c.f. [25]).

Fig. 4(a) and (b) show the single and double ionization probabilities as functions of Δt between the SA and IR-laser electric fields (2). The SA (IR) pulse has a central wavelength of 60 (800) nm and peak intensity 2×10^{13} (3×10^{14}) $\mathrm{W/cm^2}$. The value of $\omega_{SA} = 0.76$ is chosen such that it is repeatedly in resonance with the field-dressed $1s2s$ level. Note that $E^{(\mathrm{free})}_{1s,2s} = 1$ in this two-electron model. Therefore, Fig.4 (a) closely resembles in shape the $\omega_{SA} < 0.6$ result in the SAEA calculation in Fig. 3(a), and the single-ionization-probability maxima occur when the SA pulse coincides with the maxima of $|E_{IR}(t)|$.

Once released, an electron can be accelerated and driven back to the core by the IR laser field, causing non-sequential rescattering ionization of the ionic core after about 2/3 T_{IR} [26]. Hence, the single and double-ionization probabilities oscillate with the same period, $T_{IR}/2$ (Fig. 4), with maxima at almost identical delays. The double ionization probability almost vanishes for $\Delta t > 0$, since the decreasing IR laser intensity does not transfer sufficient energy to the rescattering electron to ionize the He^+ core. If the SA appears much earlier than the IR pulse ($\Delta t < -1.5T_{IR}$), the SA pulse first excites the helium atom, which is later singly and doubly ionized, once nearly maximal IR intensities are reached [27].

In conclusion, our simulations indicate that by applying a SA pulse *instantaneous* energetic shifts in singly excited He induced by a strong few-cycle IR laser pulse are mapped onto oscillations in delay-depended single ionization probabilities. We interpret these oscillations in terms of a two-step process, where excitation in the SA pulse is followed by efficient ionization out of excited states in the IR field. The excited-state population depends on the instantaneous energy gaps between the ground and excited states in the IR-laser field. Knowledge of the instantaneous energy levels in the strong IR field may lead to new schemes for the coherent control of NSDI, high harmonic generation, and molecular dissociation.

This work was supported by the NSF of China (Grant No. 10734130) and National Basic Research Program of China (Grant No. 2007CB310406, 2007CB815105), the US NSF, the Division of Chemical Sciences, Office of Basic Energy Sciences, Office of Energy Research, US DOE, and by the MEC FIS 2009- and the Ramón y Cajal Research grants.

---

[1] B.H. Bransden and C.J. Joachain, Physics of atoms and molecules (Pearson Education, Ltd, Singapore, 2003).
[2] F. H. M. Faisal, *Theory of Multiphoton Processes* (Plenum Press, New York, 1987).
[3] Shih-I. Chu and J. Cooper, Phys. Rev. A **32**, 2769 (1985).
[4] M. Dörr, R.M. Potvliege, and R. Shakeshaft, Phys. Rev. A **41**, 558 (1990).
[5] H. Rottke *et al.*, Phys. Rev. A **49**, 4837 (1994).
[6] J. Zhou *et al.*, Opt. Lett. **19**, 1149 (1994).
[7] M. Nisoli *et al.*, Opt. Lett. **22**, 522 (1997).
[8] C.G. Durfee, S. Backus, H.C. Kapteyn, and M.M. Murnane, Opt. Lett. **24**, 697 (1999).
[9] A. Apolonski *et al.*, Phys. Rev. Lett. **85**, 740 (2000).
[10] B. Schenkel *et al.*, Opt. Lett. **28**, 1987 (2003).
[11] M. Hentschel *et al.*, Nature (London) **414**, 509 (2001).
[12] J. Itatani *et al.*, Phys. Rev. Lett. **88**, 173903 (2002).
[13] M. Drescher *et al.*, Nature (London) **419**, 803 (2002).
[14] M. Uiberacker *et al.*, Nature (London) **446**, 627 (2007).
[15] A. Cavalieri *et al.*, Nature (London) **449**, 1029 (2007).
[16] E. Goulielmakis *et al.*, Nature (London) **466**, 739 (2010).
[17] P. Johnsson *et al.*, Phys. Rev. Lett. **99**, 233001 (2007).
[18] P. Ranitovic *et al.*, New J. Phys. **12**, 013008 (2010).
[19] X. M. Tong and C. D. Lin, J. Phys. B: At. Mol. Opt. Phys. **38** 2593(2005).
[20] M.R. Hermann and J.A. Fleck Jr, Phys. Rev. A **38**, 6000 (1988).
[21] We designate dressed states by *nl*, following [4], to indicate their undressed origins.
[22] E.J. Takahashi *et al.*, Phys. Rev. Lett. **99**, 053904 (2007).
[23] K.P. Singh *et al.*, Phys. Rev. Lett. **104**, 023001 (2010).
[24] F. He, A. Becker, and U. Thumm, Phys. Rev. Lett. **101**, 213002 (2008).
[25] C. Ruiz, L. Plaja, L. Roso, and A. Becker, Phys. Rev. Lett. **96**, 053001 (2006).
[26] P.B. Corkum, Phys. Rev. Lett. **71**, 1994 (1993).
[27] S. Chen, C. Ruiz, and A. Becker, Phys. Rev. A **82**, 033426 (2010).